Tacticity *versus* dimension of the extended structures in the crystals of heterospin magnets made of transition-metal complexes with the poly(aminoxyl) radical

Hiizu Iwamura,*[a] Katsuya Inoue[b] and Noboru Koga[c]

[a] *Institute for Fundamental Research in Organic Chemistry, Kyushu University, Hakozaki, Higashi-ku, Fukuoka 812-81, Japan*
[b] *Department of Applied Molecular Science, Institute for Molecular Science, Myodaiji, Okazaki 444, Japan*
[c] *Faculty of Pharmaceutical Science, Kyushu University, Maedashi, Higashi-ku, Fukuoka 812-82, Japan*

Bis- and tris(aminoxyl) radicals and di(4-pyridyl)diazomethane form crystalline complexes with extended structures upon reaction with [$M(hfac)_2$] (M = Mn^{II} or Cu^{II}, and hfac = hexafluoroacetylacetonate). Organic 2p and metal 3d spins in these complexes order at 3.4–46 K depending on the dimensions of the extended structures and the magnitude of exchange coupling between the adjacent spins. In the crystals of one-dimensional systems, the polymeric chains are isotactic in that free radical or precursor ligands and/or metal centres have the same chirality along any given chain. The polymeric chains are syndiotactic and cross link to form two-dimensional honeycomb or three-dimensional crossed parallel networks.

Organic free radicals having basic coordinating sites have been employed together with magnetic metal ions to make complexes containing organic 2p and metal 3d hybrid spins. The free-radical centers themselves may have Lewis basicity as in aminoxyl radicals and are coordinated through their oxygen atoms to magnetic metal ions such as copper(II).[1] Nitrogen bases carrying a free radical center separated from the coordination site through π-conjugated moieties may also be used. Pyridine and imidazole ligands carrying a *N-tert*-butylaminoxyl group, for example, have been synthesized to evaluate the sign and magnitude of the regiospecific magnetic interaction between the radical center and the magnetic metal ion attached to the ring nitrogen.[2]

When an organic free radical carries two ligating sites as in semiquinones and Ullman's 'nitronyl nitroxides', extended structures that are often chain polymers or macrocycles are formed with coordinatively doubly unsaturated metal ions.[3] This is schematically shown in Fig. 1(*a*). Depending on the nature of the additional interchain interactions, the chain polymers become antiferromagnets, metamagnets, or ferri/ferromagnets. By modifying and extending this design strategy to bis- and tris(aminoxyl) radicals having triplet and quartet ground states, respectively, we have been able to construct with the aid of magnetic metal ions one-dimensional (1D) chain, two-dimensional (2D) network and three-dimensional (3D) crossed parallel structures in which both the organic 2p and metallic 3d spins have been ordered in macroscopic scales.[4] Since such a rational approach by self-assembly to the tailored extended systems having relevant physical properties is of great importance in materials synthesis,[5] we have studied the crystal structures more carefully in a systematic manner to find that dimensionality of the crystal structures in these heterospin magnets is closely related to tacticity of the polymeric structures.

* Fax: +81-92-642-2735. E-mail: iwamura@ms.ifoc.kyushu-u.ac.jp
Non-SI unit employed: 1 Oe = 10^3 A m^{-1}.

Design Strategy

The design strategy for various crystal structures of given dimension from metal complexes having poly(aminoxyl) radicals as bridging ligands was as follows. π-Conjugated oligo(aminoxyl) radicals **1**–**7** have been employed as bridging ligands in which the spins of the unpaired electrons interact ferromagnetically [J(intraligand) > 0]. Dimensionality of the complex as well as sign and magnitude of the exchange coupling between the neighboring spins may be readily tuned in this strategy.[6] A bis(monodentate) diradical with a triplet ground state (S = 1), *e.g.*, **1**,[7] would form with coordinatively doubly unsaturated metal ions a 1:1 complex having a 1D infinite chain structure [Fig. 1(*b*)]. Since the exchange coupling between the ligands and the directly attached transition-metal ions is typically antiferromagnetic [J(coordination) ≪ 0] and the 2p and 3d spins tend to cancel each other out, a residual spin would be established for the repeating unit unless the spin of the latter is unity. Such a 1D array of spins would become an antiferro-, meta-, or ferromagnet depending on the nature of the interchain interaction. Since the interaction between the 1D chains is much weaker compared with the intrachain interaction, the critical temperatures (T_C) for exhibiting macroscopic ordering of the spins will consequently be very low. For a triplet diradical such as the bis(aminoxyl) radical **2**[4d] in which each radical center can serve as a bis(monodentate) bridging ligand, complexation would give rise to a ladder polymer as in Fig. 1(*c*). The spin ordering in these systems should be less vulnerable to defects than that in purely 1D systems because there will be a detour available for the exchange coupling through bonds between the two parts of the polymer molecule separated by a chemical defect. The tris(monodentate) diradical **3**[4g] with a doublet ground state and triradicals **4**–**6**[4f,7c] with quartet ground states ($S = \frac{3}{2}$) in which the radical centers are arranged in a triangular disposition would form 3:2 complexes with coordinatively doubly unsaturated 3d metal ions M. In an ideal case, a 2D hexagonal network structure would be generated [Fig. 1(*d*)].

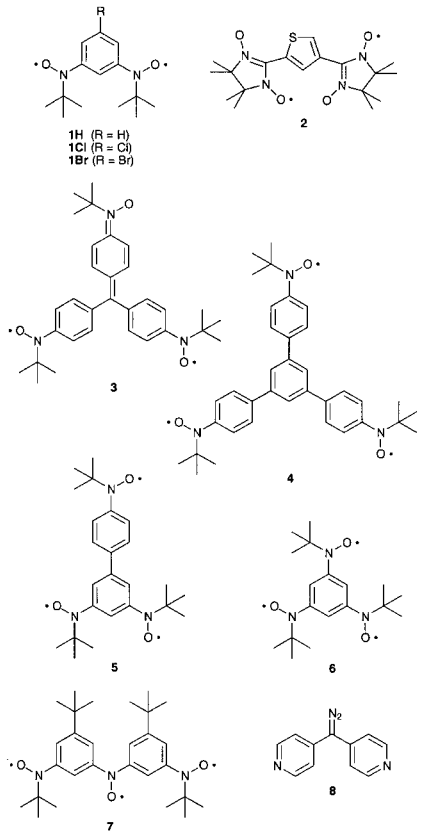

A T-shaped quartet triradical carrying two inequivalent ligating sites, *e.g.*, **7**[8] would form a 1D chain by using two terminal aminoxyl groups. The middle aminoxyl group might then be used to cross-link the chains to form a 2D [Fig. 1(*e*)] or a 3D network structure [Fig. 1(*e'*)] depending on whether or not the second bridging takes place between the same chains as cross-linked by the first bridging. The spin alignment in these systems would be very much stabilized and is expected to give higher-T_C magnets.

A dipyridine base carrying a diazo group that is separated from the base centers through a π-conjugated framework and can generate a triplet carbene center by photolysis is represented by **8**.[9]

Experimental

Preparation of the 3d transition-metal–poly(aminoxyl) radical complexes

A suspension of manganese(II) bis(hexafluoroacetylacetonate) dihydrate, $[Mn(hfac)_2 \cdot 2H_2O]$, in n-heptane was refluxed to remove water of hydration by azeotropic distillation. To the resulting cooled solution were added **1H**[7] in n-heptane. The mixture was concentrated under reduced pressure to give black needles of $[Mn(hfac)_2 \cdot \mathbf{1H}]$ from a deep brown solution.[4b]

The reaction of $[Mn(hfac)_2]$ with the tris(aminoxyl) radical **7**[8] was complex; while an equimolar mixture in diethyl ether containing n-hexane at −10 °C gave black blocks of the 1 : 1 complex $[Mn(hfac)_2 \cdot \mathbf{7} \cdot n\text{-}C_6H_{14}]$,[4c] a mixture containing $[Mn(hfac)_2]$ in 1.7 molar excess in n-heptane–diethyl ether (2 : 3) gave black blocks of the 3 : 2 complex $[\{Mn(hfac)_2\}_3 \cdot \mathbf{7}_2]$ in 10 d at 0 °C.[4e]

The complex $[\{Mn(hfac)_2\}_3 \cdot \mathbf{4}_2 \cdot n\text{-}C_7H_{16}]$[4a] was obtained by dissolving $[Mn(hfac)_2 \cdot 2H_2O]$ in a mixture of diethyl ether, n-heptane and benzene followed by addition of **4**[7c] in benzene. Black blocks were formed from a deep violet solution.

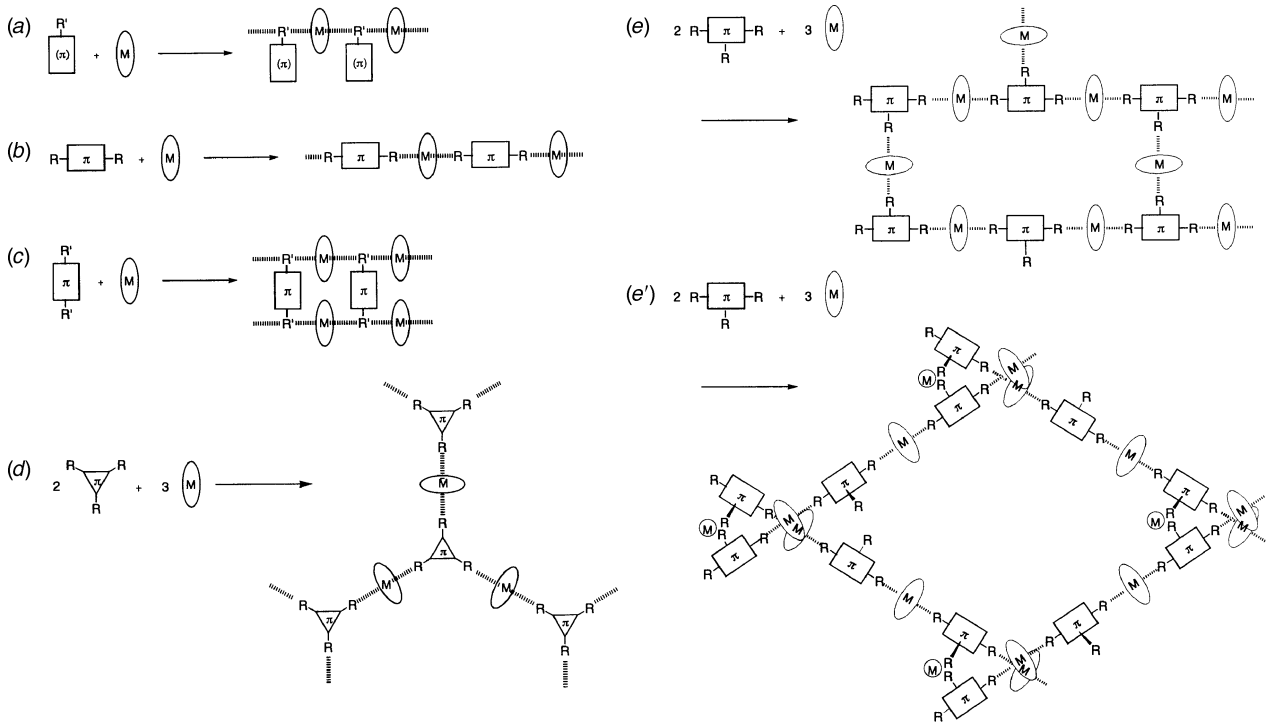

Fig. 1 Design strategy for the construction of 3d transition-metal ion (M)–free radical (**R** and **R'**) complexes having prescribed structures: (*a*) 1D chains or macrocycles from a bis(monodentate) monoradical and (*b*) a triplet diradical; (*c*) ladder polymers from triplet bis{bis(monodentate)} diradicals; (*d*) 2D network sheets from tris(monodentate) quartet triradicals; and (*e*) 2D networks or (*e'*) 3D crossed parallels from tris(monodentate) quartet triradicals depending on where the second bridging takes place

While $[Mn(hfac)_2]$ gave similar black violet 3 : 2 complexes with the tris(aminoxyl) radical **5**[4f] and bis(aminoxyl) radical **3**[4g], **6**[7c] did not form any complex probably because of steric congestion around the ligand molecule. The diradical **2** gave with $[Mn(hfac)_2]$ dark green powders of the complex $[\{Mn(hfac)_2\}_3 \cdot \mathbf{2}_2 \cdot CH_2Cl_2]$; the expected 2 : 1 complex was not obtained.[4d]

A 1 : 1 complex $[Mn(hfac)_2 \cdot \mathbf{8}]$ was obtained as orange bricks from a solution of $[Mn(hfac)_2]$ and **8**[9] in n-heptane–CH_2Cl_2 (1 : 1) containing a small amount of methanol.[10] Dark greenish brick-like crystals of $[Cu^{II}(hfac)_2 \cdot \mathbf{8}]$ were obtained similarly in benzene–CH_2Cl_2–CH_3OH (1 : 1 : 0 · 1).

Crystallography

The X-ray crystal data of the manganese complexes of the aminoxyl radicals **1**, **4** and **7** are collected in Table 1. The crystal structural features are described below. Neither $[\{Mn^{II}(hfac)_2\}_3 \cdot \mathbf{2}_2 \cdot CH_2Cl_2]$[4d] nor $[\{Mn^{II}(hfac)_2\}_3 \cdot \mathbf{3}_2]$[4f] gave good single crystals amenable to X-ray crystal structure analysis. Reduced symmetry of **5** relative to C_3 of **4**, appears to be responsible for a failure to give good single crystals of $[\{Mn(hfac)_2\}_3 \cdot \mathbf{5}_2]$ for X-ray analysis.

CCDC reference number 440/009.

Magnetic measurements. Magnetic data of the poly(aminoxyl) radical ligand and the heterospin complexes were determined on a Quantum Design MPMS2 SQUID susceptometer unless otherwise stated. High-field data ($H > 10\,000$ Oe) were obtained on an Oxford Instruments Faraday magnetic balance system with a 7 T superconducting magnet.

Results and Discussion

X-Ray crystal and molecular structures of the complexes

$[Mn^{II}(hfac)_2 \cdot \mathbf{1}]$. The manganese(II) ion in $[Mn(hfac)_2 \cdot \mathbf{1}]$[4b] has an octahedral coordination with four oxygen atoms of two hfac anions and two oxygen atoms of two aminoxyl groups from two different diradical molecules of **1** in *cis* configuration. It is noted that the resulting 1D polymeric chain is isotactic in that each ligand molecule of **1** has the same chirality, *i.e.*, *R* or *S*, in a given chain (Fig. 2). The chains are also isotactic with respect to the Δ and Λ chirality of the octahedral Mn^{II} centers. The second isotactic chain lying along the crystal *b* axis has opposite chirality to the first one; there is no net chirality exhibited by the crystals themselves. The strongest interchain coupling is expected for the $N(Bu^t)O^{\cdot}\cdots F\cdots N(Bu^t)O^{\cdot}$ interaction having distances of 4.95 Å on the one hand and 4.97 Å on the other. This type of interaction is suggested to be antiferromagnetic as dictated by the McConnell's[11a] theory and the superexchange mechanism through the fluorine atom. Since the Mn^{II} ion is *cis* coordinated with two radical oxygens, the 1D chain is folded like an α-helix of peptides to make either a right-handed or left-handed helix with a pitch corresponding to two $[Mn(hfac)_2 \cdot \mathbf{1}]$ units.

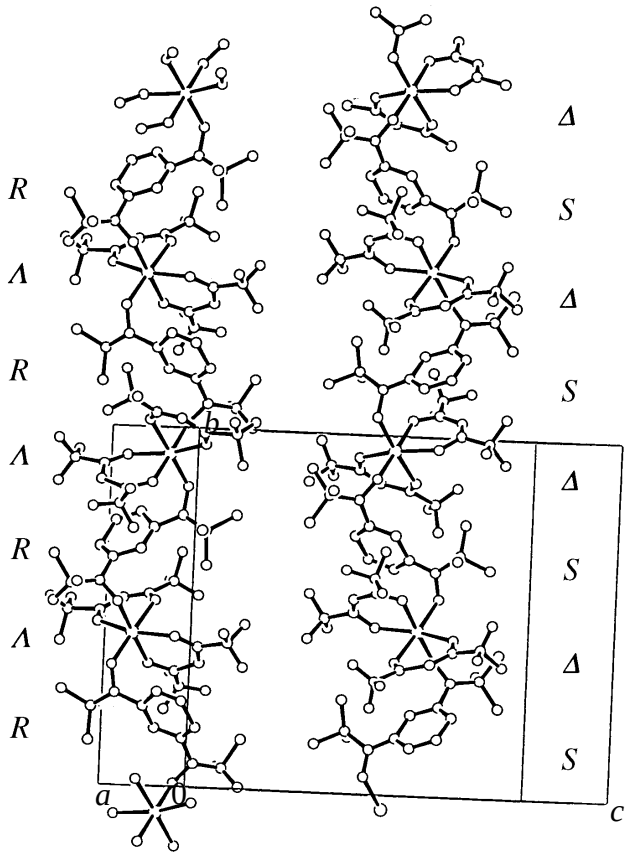

Fig. 2 The 1D chains of $[Mn^{II}(hfac)_2 \cdot \mathbf{1H}]$ extending along the *b* axis

$[\{Mn^{II}(hfac)_2\}_3 \cdot \mathbf{4}_2 \cdot \text{n-}C_7H_{16}]$. The Mn^{II} ion in the complex $[\{Mn(hfac)_2\}_3 \cdot \mathbf{4}_2 \cdot \text{n-}C_7H_{16}]$ has an octahedral coordination with four equatorial oxygen atoms of two hfac anions and two

Table 1 Crystallographic data for the manganese(II) complexes $[Mn(hfac)_2 \cdot \mathbf{1H}]$, $[\{Mn(hfac)_2\}_3 \cdot \mathbf{4}_2 \cdot \text{n-}C_7H_{16}]$, $[Mn(hfac)_2 \cdot \mathbf{7} \cdot \text{n-}C_6H_{14}]$ and $[\{Mn(hfac)_2\}_3 \cdot \mathbf{7}_2]$

Chemical formula	$C_{24}H_{24}N_2O_6F_{12}Mn$	$C_{102}H_{90}N_6O_{18}F_{36}Mn_3 \cdot C_7H_{16}$	$C_{86}H_{90}N_6O_{18}F_{36}Mn$	$C_{38}H_{44}N_3O_7F_{12}Mn \cdot C_6H_{14}$
a/Å	9.212(3)	28.462(7)	10.137(3)	17.82(1)
b/Å	16.620(3)	—	19.426(5)	24.367(4)
c/Å	20.088(2)	18.40(1)	27.187(7)	12.522(2)
β/°	—	98.46(1)	95.21(2)	—
U/Å^3	3042(1)	12914(8)	5331(2)	5436(4)
Z	4	4	4	2
Formula weight	719.38	2636.82	1023.88	2344.44
Space group	$P2_1/n$ (No. 14)	$R3(h)$ (No. 148)	$P2_1/c$ (No. 14)	$Pnn2$ (No. 34)
T/°C	21	22	21	22
λ/Å	0.71069	0.71069	0.71069	0.71069
r_{calc}/g cm^{-3}	1.571	1.356	1.275	1.432
$R(F)$	0.055	0.090	0.098	0.180
$R_W(F)$	0.058	0.112	0.096	0.108

axial oxygen atoms of two aminoxyl groups from two different molecules of **4**.[4a] Six triradical molecules and six Mn ions make an expanded hexagon from which an extended hexagonal network is constructed by sharing its edges (Fig. 3). A disordered n-heptane molecule is contained in each hexagonal cavity. The 2D network sheets form a graphite-like layered structure in which a mean interlayer distance is only 3.58 Å and the adjacent layers have slipped in the *ab* plane by a length of the edge of the hexagon from the superimposable disposition. As a result, any middle benzene ring of **4** stacks with the corresponding ring on the next layer rotated by 60° along the C_3 axis. On the basis of the spin density, phase of the π-electron polarization, and interatomic distance,[11] the strongest ferromagnetic interlayer exchange interaction is found between the outer benzene ring carbon of **4** *para* to the aminoxyl group on one layer and the *meta* carbon on the next layer at a distance of 3.78 Å.

Three *p*-(*N*-oxyl-*N*-*tert*-butylamino)phenyl groups in **4** are tilted out of the middle 1,3,5-trisubstituted benzene ring plane by 33(2)° to make a chiral propeller with a C_3 axis. We note that the chirality of the six molecules of **4** alternates as *R*-*S*-*R*-*S*-*R*-*S* in any giant hexagon of the crystal structure of complex $[\{Mn^{II}(hfac)_2\}_3 \cdot \mathbf{4}_2 \cdot n\text{-}C_7H_{16}]$. If the chirality along the hexagon were isotactic, *i.e.*, *R*-*R*-*R*-*R*-*R*-*R* or *S*-*S*-*S*-*S*-*S*-*S*, both ends of the hexamer could not have closed to make a hexagon; a large helical ladder might have been formed instead as in single-strand DNA.

$[Mn^{II}(hfac)_2 \cdot \mathbf{7} \cdot n\text{-}C_6H_{14}]$. The manganese(II) ion has an octahedral coordination with the four oxygen atoms of two hfac anions and the two oxygen atoms of the terminal aminoxyl groups of two different molecules of **7**. A 1D zigzag chain formed by alternation of the manganese ion and triradical **7** is isotactic in that each molecule of **7** has the same C_2 chirality, *i.e.*, *R* or *S*, in a given chain. There is an enantiomeric pair of the isotactic chains in the unit cell (Fig. 4).[4c] Since the Mn^{II} ion is *trans* coordinated with the radical oxygens, the 1D chain is not folded but extended as in a β-sheet structure of peptides. The middle aminoxyl radicals of **7** in the adjacent chains are out of phase and do not take part in the coordination with any additional manganese ion and, as a result, do not form the extended β-sheet structure.

A disordered n-hexane molecule is contained in each unit cell. On the basis of the spin density known to be largely localized on the N—O moieties and the observed intermolecular distances between them, the strongest interchain interaction is judged to arise from the $N(Bu^t)O^{\cdot}\cdots N(Bu^t)O^{\cdot}$ interaction with distances of 4.86 Å between the neighboring chains and estimated to be antiferromagnetic.[11c]

$[\{Mn^{II}(hfac)_2\}_3 \cdot \mathbf{7}_2]$. A crossed parallel-shaped three-dimensional polymeric network is formed in an orthorhombic crystal of $[\{Mn^{II}(hfac)_2\}_3 \cdot \mathbf{7}_2]$ (Fig. 5).[4e] Oxygen atoms of the terminal aminoxyl groups of triradical **7** are ligated to two different manganese ions to form a 1D chain in the *bc* plane of the crystal. Since any manganese ion in an octahedral position is attached to two aminoxyl oxygens from two different triradical molecules in a *trans* disposition, the tris(aminoxyl) molecules are in zigzag orientation along the chain. The *N*,*N*-diarylaminoxyl unit is in a chiral C_2 conformation and the *R* and *S* forms alternate along the chain to make it syndiotactic. The middle aminoxyl group of the ligand molecule **7** on one chain is used to link its oxygen with that in the adjacent chains extended in the $b/-c$ diagonal direction through a third Mn^{II} ion in an octahedral position. The two aminoxyl oxygens are in *cis* configuration and the two chains are bridged with the intersecting mean angle of 54.4°, establishing a crossed-parallel shaped 3D polymeric network. It is noted that the bridging between the neighboring chains takes place between the ligand molecules **7** of the same chirality; two molecules of **7** in *R* configuration are bridged through the Λ Mn^{II} complex, and *vice versa*.

The crossed parallel structure seems unique but it is noted that the structure found here is similar to a three-connected net found in the silicon sublattice of $ThSi_2$ [Fig. 6(*a*)]. In this trigonal net, parallel chains extending in the *x* direction are in phase on a given *xy* plane and orthogonal to those extending in the *y* direction on the next *xy* planes shifted in the $\pm z$ direction. The sublattice consists of a motif of trimethylenemethane in which one CH_2 group extending in the *z* direction is orthogonal to the rest of the molecular repeating

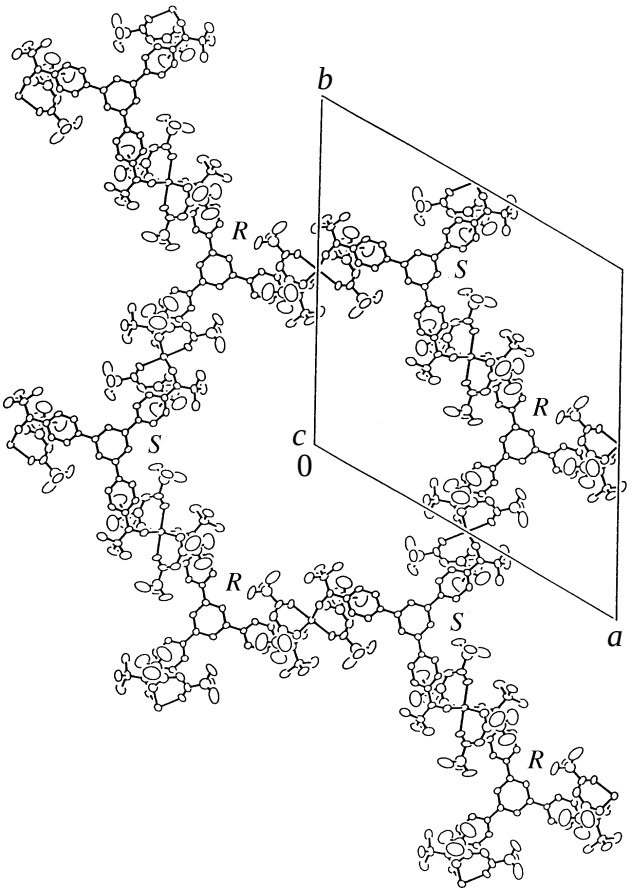

Fig. 3 The complex $[\{Mn^{II}(hfac)_2\}_3 \cdot \mathbf{4}_2 \cdot n\text{-}C_7H_{16}]$ viewed down the *c* axis, showing the formation of 2D hexagonal nets. The $n\text{-}C_7H_{16}$ molecules are disordered and not shown

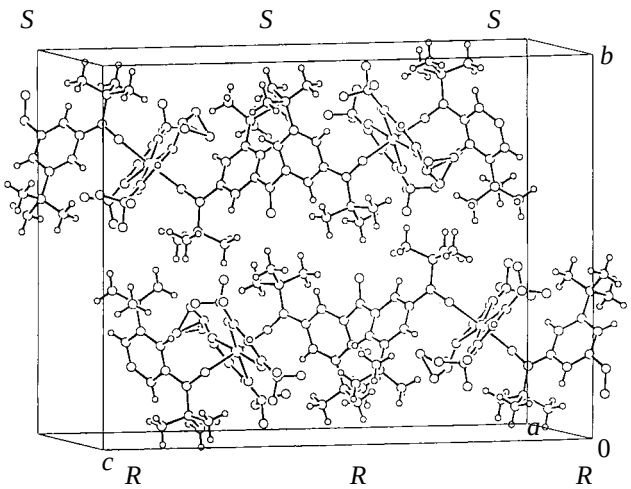

Fig. 4 A view approximately down the *a* axis of an enantiomeric pair of isotactic 1D chains of $[Mn^{II}(hfac)_2 \cdot \mathbf{7} \cdot n\text{-}C_6H_{14}]$. Molecules of $n\text{-}C_6H_{14}$ are not shown for clarity

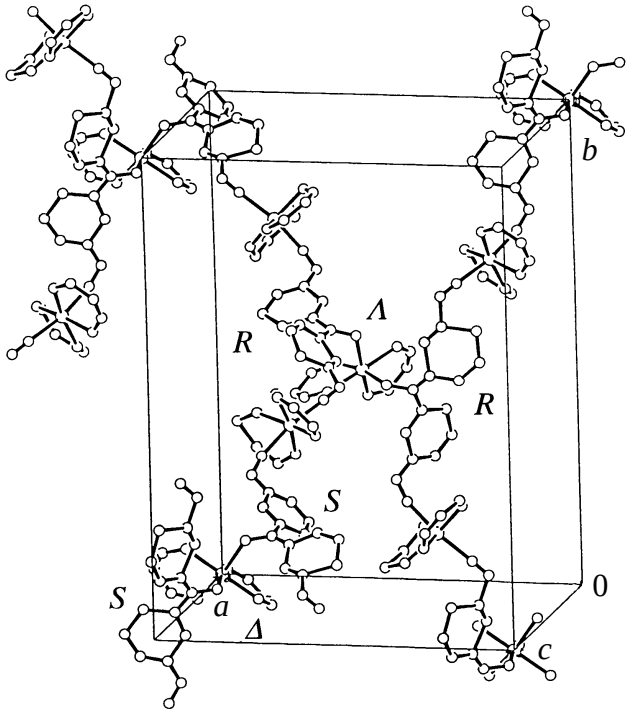

Fig. 5 3D crossed parallel structure of $[\{Mn^{II}(hfac)_2\}_3 \cdot \mathbf{7}_2]$. The CF_3 and $(CH_3)_3C$ groups are not shown for clarity

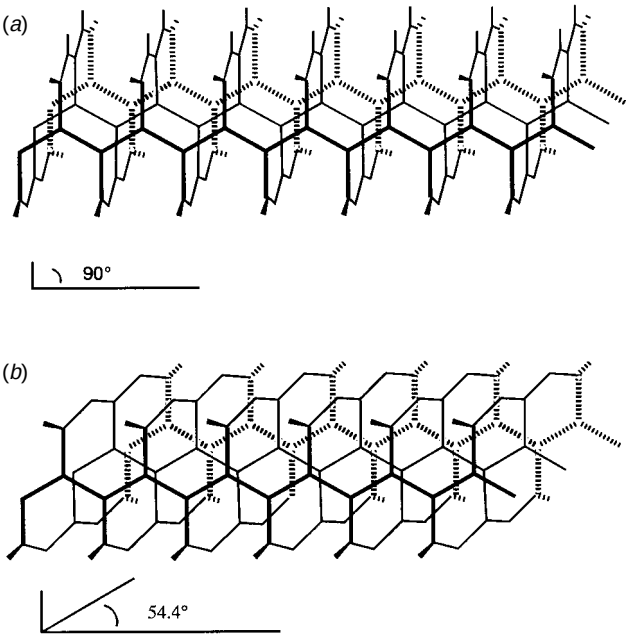

Fig. 6 Schematic drawing of the three-connected nets for (*a*) $ThSi_2$ and (*b*) $[\{Mn^{II}(hfac)_2\}_3 \cdot \mathbf{7}_2]$. One CH_2 group in the trimethylenemethane-type motifs is orthogonal and tilted by 54.4° in (*a*) and (*b*), respectively

units on the *xy* plane. In graphite the entire three-connected net is planar.[12] When the dihedral angle in the trimethylenemethane motif is *ca.* 54.4°, the sublattice is squeezed into another as shown in Fig. 6(*b*). This structure is exactly what is observed in the crossed parallel structure of the complex $[\{Mn^{II}(hfac)_2\}_3 \cdot \mathbf{7}_2]$. The crystal is expected to be isotropic in the *xy* direction but anisotropic in the *z* direction by symmetry. It is also noted that, along a given chain extending in the direction parallel to the *xy* plane, torsion of the CH_2 unit with respect to the axis parallel to the *z* axis alternates between +54.4° and −54.4°, showing that the 1D chain should be syndiotactic by symmetry.

$[Mn^{II}(hfac)_2 \cdot \mathbf{8}]$. The quality of the single crystals has not enabled refinement of the X-ray crystal structure of $[Mn^{II}(hfac)_2 \cdot \mathbf{8})]$ ($R = 0.244$, $R_W = 0.121$) and yet is enough to support the formation of a helical 1D chain in which the two pyridyl nitrogens of a molecule of **8** are ligated to two different manganese(II) ions and each Mn ion is coordinated with two pyridyl nitrogens in a *cis* configuration (Fig. 7).[9] The chain is isotactic with respect to the chirality of the C_2 molecules of **8** as well as the octahedral Mn^{II} complexes. Like an α-helix of peptides, the one-dimensional chain is folded to make a helix with a pitch corresponding to two $[Mn(hfac)_2 \cdot \mathbf{8}]$ units.

Magnetic properties

Ferromagnetic intraligand coupling in the poly(aminoxyl) radical ligands. The magnitude of the exchange coupling (J_{intra}) between the aminoxyl radicals in the ligand bis- and tris(aminoxyl) radicals **1**–**7** before complex formation was studied by means of the temperature dependence of their molar magnetic susceptibility, χ_M, and analyzed using the Bleaney–Bowers-type equations.[7c,8,13,14] We note from all the positive J_{intra} values (Table 2) that the aminoxyl radical centers are connected by the right topology for ferromagnetic coupling within each molecule. Since the low-spin excited states could not be populated thermally, only the lower limits of J_{intra} values were obtained for **1** and **6**. It is noted that the J_{intra} values decrease as the number of the intervening benzene rings increases; polarization of the π electrons on the benzene rings is gradually attenuated as the distance between the radical sites increases through increasing numbers of bonds.

When photolyzed in MTHF solid solution, radical **8** gave the corresponding triplet carbene, which had zero-field splitting parameters $|D/hc| = 0.434$ and $|E/hc| = 0.020$ cm^{-1} [9,10b] and started to disappear at 60–80 K, as observed by EPR spectroscopy.

Magnetic susceptibility and magnetization of metal complexes. Magnetic data of the heterospin complexes were analyzed[15] on the basis of their crystal structures described above. The results are summarized in Table 3 and discussed in some detail when relevant structural data are available.

1D complex $[Mn^{II}(hfac)_2 \cdot \mathbf{1}]$. Temperature dependence of χ_M for $[Mn(hfac)_2 \cdot \mathbf{1H}]$ at 5000 Oe gave a Curie constant *C* of 1.9 cm^3 K mol^{-1} and a Weiss constant θ of 40 K in the range

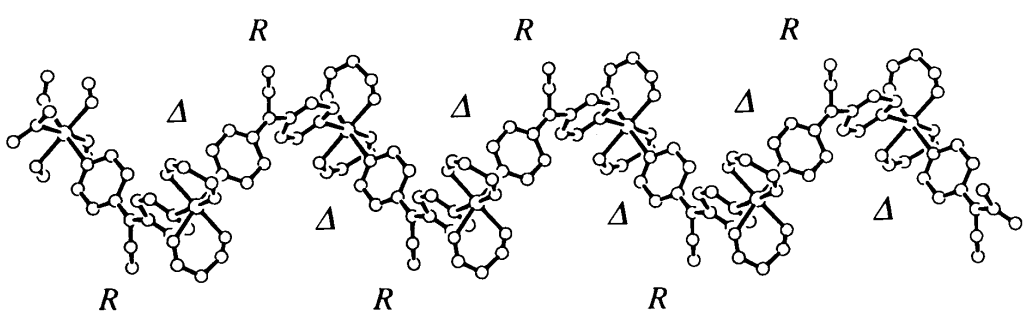

Fig. 7 View of an unrefined 1D helical chain of $[Mn^{II}(hfac)_2 \cdot \mathbf{8}]$

Table 2 Magnitude of the intraligand exchange coupling (J_{intra}) between the nitroxide radicals **1**–**7**

Aminoxyl radical	J_{intra}/k_B(K)	θ/K	Sample morphology	Ref.
1	⩾300	−7.8	Orange crystals	8
2	+80 ± 4	−0.04 ± 0.02	Black block crystals	4(*d*)
3	⩾300		Red-purple crystals	4(*g*)
4	+6.8 ± 0.1	−2.13 ± 0.04	Red crystals	7(*c*)
4	+5.3 ± 0.1		Isolated in Tween 40	7(*c*)
5	≈300, +67 ± 5		Isolated in PVC	4(*f*)
6	⩾300		Reddish yellow crystals	7(*c*)
7	+240 ± 20	−19 ± 2	Orange crystals	8

50–350 K.[4b] An observed $\chi_M T$ value of 2.11 cm^3 K mol^{-1} at 300 K is slightly but not much larger than a theoretical value of 1.88 cm^3 K mol^{-1} for a model in which the interaction between the Mn^{II} and the directly attached aminoxyl radical is antiferromagnetic ($J_{coord}/k_B < -300$ K) and the two spins within the molecule of **1H** are not yet fully aligned ($J_{intra} \leqslant$ 300 K). The $\chi_M T$ value increased steadily, reached a maximum at 8.5 K, and then decreased with decreasing temperature. The zero-field cooled (ZFC) magnetization measured at 0.5 Oe after cooling down without applied field also showed a sharp cusp at 5.5 K, suggesting the development of a higher order antiferromagnetic interaction. The magnetization at 1.8 K revealed metamagnetic behavior; while the characteristic behaviour for an antiferromagnet, namely, an insensitive response of the magnetization to the weak applied magnetic field, was observed below *ca.* 200 Oe, a sharp rise and approach to saturation of magnetization characteristic of a ferromagnet was observed at higher applied magnetic field (Fig. 8). Any meaningful interchain interaction is estimated to be due to the antiferromagnetic superexchange between the two aminoxyl centers on the adjacent chains through the fluorine atom (*vide supra*). The complex underwent transition to a metamagnet at 5.5 K;[4b] below this temperature it behaved as an antiferromagnet, but the magnetization increased sharply and became readily saturated at fields higher than 200 Oe.

Temperature dependencies of $\chi_M T$ of the complexes of $Mn(hfac)_2$ with **1Cl** and **1Br** were similar to that of $[Mn(hfac)_2 \cdot \mathbf{1H}]$.[4h] The magnetization at 1 Oe revealed that the halogen-containing complexes underwent transition into ordered states at 1.8 K. Saturation magnetization values (M_{sat}) approaching 3 μ_B were obtained at 1.8 K and 30 000 Oe in the three $[Mn(hfac)_2 \cdot \mathbf{1}]$ complexes in good agreement with the antiferromagnetic coupling [$J_{coord} < 0$ and $M_{sat} = 3$ μ_B ($\frac{5}{2} - \frac{2}{2} = \frac{3}{2}$)] between the manganese(II) ion and triplet **1**.

3 : 2 *Complex* $[\{Mn^{II}(hfac)_2\}_3 \cdot \mathbf{2}_2 \cdot CH_2Cl_2]$ *with a potential ladder polymer structure.* The complex $[\{Mn^{II}(hfac)_2\}_3 \cdot \mathbf{2}_2 \cdot CH_2Cl_2]$ is still deficient in the amount of the metal ions for a 2 : 1 ladder polymer [Fig. 1(*c*)], indicating that the radical sites are not fully ligated with the manganese ions. While a transition to a magnet was found at 11 K, the

Table 3 Complexes of $[Mn(hfac)_2]$ with bis- and tris(aminoxyl) radicals

Ligands L	Composition Mn : L	Magnetism	Magnetic phase transition T_C/K	Ref.
1H	1 : 1	Metamagnetic	5.5	4(*b*)
1Cl	1 : 1	Ferri/ferromagnetic	5.2	4(*h*)
1Br	1 : 1	Ferri/ferromagnetic	5.0	4(*h*)
2	3 : 2	Ferri/ferro magnetic	11	4(*d*)
3	3 : 2	—	—	4(*g*)
4	3 : 2	Ferri/ferromagnetic	3.4	4(*a*)
5	3 : 2	Ferri/ferromagnetic	9.5	4(*f*)
7	1 : 1	Metamagnetic	11	4(*c*)
7	4 : 3	Ferri/ferromagnetic	32	4(*i*)
7	3 : 2	Ferri/ferromagnetic	46	4(*e*)

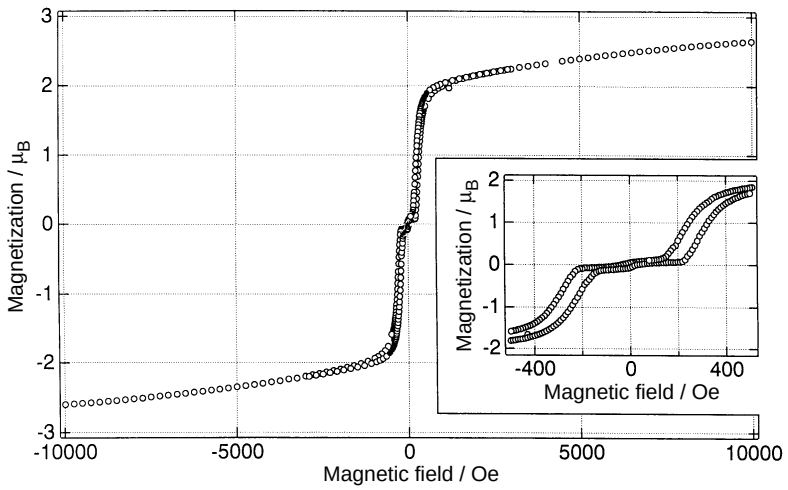

Fig. 8 Field dependence of the magnetization of $[Mn^{II}(hfac)_2 \cdot \mathbf{1H}]$ measured at 1.8 K

observed magnetization curve which consisted of extremely field-sensitive and slowly saturating parts suggested that only *ca.* 30% of the unpaired electrons in this powder sample align spontaneously below the critical temperature. The rest of the spins appear to be independent or form less ordered segments.

2D Complex [$\{Mn(hfac)_2\}_3 \cdot \mathbf{4}_2 \cdot n\text{-}C_7H_{16}$]. The $\chi_M T$ *vs.* T plot for the complex [$\{Mn^{II}(hfac)_2\}_3 \cdot \mathbf{4}_2 \cdot n\text{-}C_7H_{16}$] at a field of 5000 Oe gave a minimum at *ca.* 115 K (Fig. 9, inset).[4a] The observed μ_{eff} value $\{=(3k\chi_M T/N)^{\frac{1}{2}}\}$ of 6.7 μ_B at this temperature is in good agreement with a model in which the interaction between the Mn^{II} and the aminoxyl group directly attached to it is antiferromagnetic and the three spins within a molecule of **4** are not yet aligned. The $\chi_M T$ values increased with decreasing temperature and showed a maximum at 2.5 K. When the measurement was carried out in a much lower field of 1 Oe, magnetization values showed a sharp rise at $T_C = 3.4$ K (Fig. 9). Spontaneous magnetization was observed below T_C, demonstrating a transition to a bulk magnet. Magnetization values of the complex below T_C decreased at lower temperature, probably due to the immobilization of the domain walls.[16] The magnetization reached nearly 9 μ_B at 30,000 Oe at 1.8 K, in good agreement with a model having an antiferromagnetic interaction between the Mn^{II} and **4** ($J_{coord} < 0$), ($M_{sat} = 9\ \mu_B = \frac{5}{2} \times 3 - \frac{3}{2} \times 2 = \frac{9}{2}$). A hysteresis loop at 2 K consisted of the remnant magnetization of 53.9 cm^3 G mol^{-1} and the coercive field of 3.8 Oe.

While perfect 2D network sheets with ferro- ($J_{intra} > 0$) and antiferro-magnetic ($J_{coord} < 0$ K) coupling together with ferromagnetic stacking of the layers have been obtained, the observed T_C of the ferro/ferrimagnet was not as high as expected for such a high-dimensional structure. This is ascribed to a weak intramolecular coupling ($J_{intra}/k_B = 6.8$ K) among the three aminoxyl units in the molecule of **4**.[7c] Any triradical that has three aminoxyl groups arranged in a triangular fashion with a larger J_{intra} value should have a higher T_C value. A complex of the tris(aminoxyl) radical **5** which has stronger ferromagnetic interactions (see Table 3), has therefore been tested. The T_C value rose to 9.5 K indeed in black blocks of [$\{Mn(hfac)_2\}_3 \cdot \mathbf{5}_2$].[4f]

1D [$Mn(hfac)_2 \cdot \mathbf{7} \cdot n\text{-}C_6H_{14}$]. The $\chi_M T$ value of 2.42 cm^3 K mol^{-1} at 300 K is slightly larger than a theoretical value of 2.25 for antiparallel spins of two $\frac{1}{2}$ spins of organic radicals and one $\frac{5}{2}$ spin of a d^5 Mn^{II} ion and a non-interacting $\frac{1}{2}$ spin of the middle aminoxyl moiety.[4c] The $\chi_M T$ value decreased with decreasing temperature and started to increase after reaching a minimum at 114 K [Fig. 10 (inset)]. When magnetization was measured in a much lower field, it showed a sharp rise at 11 K and then decreased with decreasing temperature (Fig. 10). The appearance of an interchain interaction is suggested. The ZFC magnetization also showed a sharp cusp at *ca.* 11 K. The magnetization at 1.8 K revealed metamagnetic behavior.

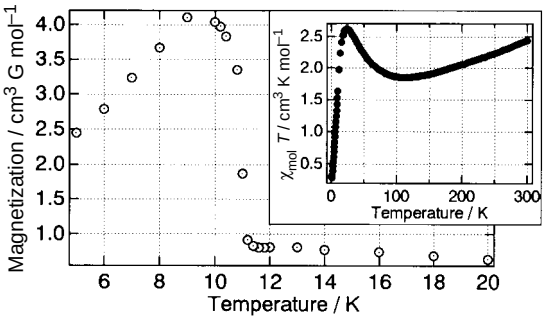

Fig. 10 Temperature dependence of magnetization for the complex [$Mn^{II}(hfac)_2 \cdot \mathbf{7} \cdot n\text{-}C_6H_{14}$] measured at a magnetic field of 5 Oe. The inset shows a plot of $\chi_M T$ vs. T

3D [$\{Mn^{II}(hfac)_2\}_3 \cdot \mathbf{7}_2$] *with a high* T_C *of* 46 K. A μ_{eff} value of 8.31 μ_B at 300 K and 5000 Oe is larger than the theoretical value of 6.71 μ_B expected for a short-range antiferromagnetic ordering of six $\frac{1}{2}$ spins for **7** and three $\frac{5}{2}$ spins for the d^5 Mn^{II} ion in [$\{Mn(hfac)_2\}_3 \cdot \mathbf{7}_2$].[4e] As T was lowered, μ_{eff} increased monotonically in proportion to the increase in the correlation length within the network. Together with the lack of a minimum at lower temperature, the room temperature μ_{eff} value suggests strong antiferromagnetic coupling ($J_{coord}/k_B < -300$ K) between the Mn^{II} ion and the aminoxyl radical of **7** in which the 2p spins of the three unpaired electrons are partly coupled ferromagnetically ($J_{intra}/k_B \geqslant 240$ K). In the low-temperature range, the magnetic behavior is qualitatively equivalent to a three-dimensional ferromagnetically coupled network of $S = \frac{3}{2}$ spins consisting of the $S(\frac{1}{2})$–$S(\frac{5}{2})$–$S(\frac{1}{2})$ units. The temperature dependence of the magnetization M for a polycrystalline sample of [$\{Mn(hfac)_2\}_3 \cdot \mathbf{7}_2$] was investigated at 5 Oe; upon cooling the FC magnetization of the sample showed an abrupt rise at $T_C = 46$ K (Fig. 11).

The field dependence of the magnetization at 5 K showed two important features.[4e] First, the magnetization rose sharply at low field, reached a value of *ca.* 9 μ_B (50 000 cm^3 G mol^{-1}) at 220 Oe and became saturated. The saturation value is in good agreement with a theoretical M_{sat} of 9 μ_B ($\frac{5}{2} \times 3 - \frac{3}{2} \times 2 = \frac{9}{2}$) expected for the antiferromagnetic ordering between

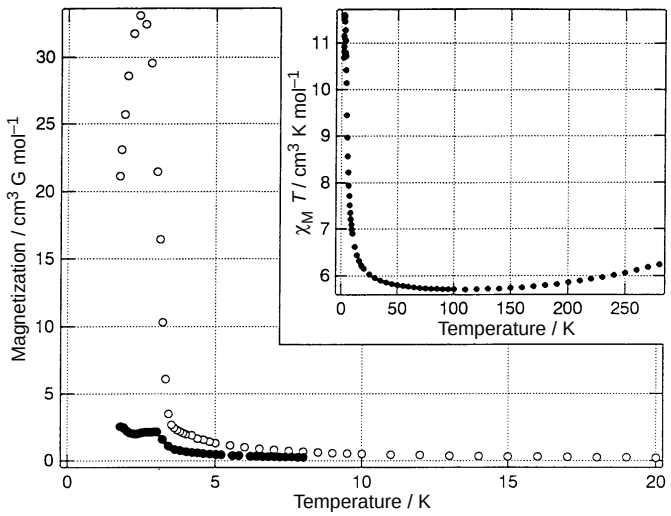

Fig. 9 Magnetization *vs.* T plots for the complex [$\{Mn^{II}(hfac)_2\}_3 \cdot \mathbf{4}_2 \cdot n\text{-}C_7H_{16}$] measured at a magnetic field of 1 Oe (○) and spontaneous magnetization (●). The inset shows $\chi_M T$ *vs.* T plots for the complex measured at 5000 Oe

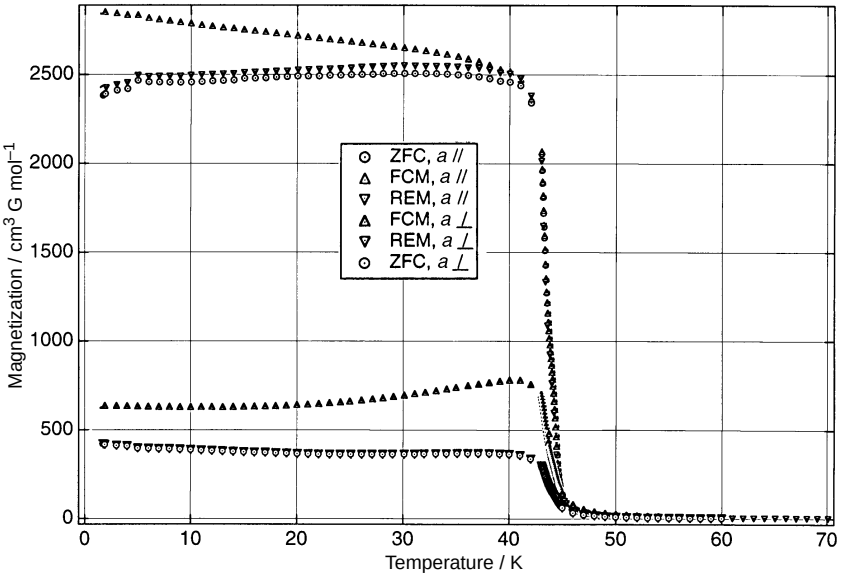

Fig. 11 Temperature dependence of zero-field cooled (ZFC), field-cooled (FCM), remanent (REM) magnetization of $[\{Mn^{II}(hfac)_2\}_3 \cdot \mathbf{7}_2]$. The applied field is parallel or perpendicular to the *a* axis

the d^5 Mn^{II} ion and $S = \frac{3}{2}$ triradical **7**. Secondly, a conspicuous magnetocrystalline anisotropy was found in which the easy axis of magnetization lies along the *a* axis of the crystal lattice and the hard axis lies perpendicular to it (Fig. 11).

3 : 2 *Complex* $[\{Mn^{II}(hfac)_2\}_3 \cdot 3_2]$. A Curie constant $C = 7.86$ cm^3 K mol^{-1} and a Weiss temperature $\theta = 87.5$ K in $[\{Mn^{II}(hfac)_2\}_3 \cdot \mathbf{3}_2]$[4g] revealed the occurrence of ferromagnetic interaction. Failure to detect a magnetic transition to an ordered phase is ascribed to disorder in the solid sample.

1D *Complex* $[Mn(hfac)_2 \cdot \mathbf{8}]$ *before and after irradiation.* Before irradiation, $\chi_M T$ values of a fine crystalline sample of $[Mn(hfac)_2 \cdot \mathbf{8}]$ were nearly constant at 2–300 K. A value of 4.14 cm^3 K mol^{-1} at 300 K is close to a theoretical spin-only value of 4.37 cm^3 K mol^{-1} expected for a dilute paramagnet of $S = \frac{5}{2}$. When irradiated with a xenon lamp ($\lambda > 400$ nm) at *ca.* 9 K, $\chi_M T$ values changed with irradiation time and a constant value was reached after 18 h (Fig. 12). As the temperature was increased from 2 to 300 K in the dark after the photolysis, $\chi_M T$ values increased, reached a maximum of 32.2 cm^3 K mol^{-1} at 3 K, rapidly decreased to a shallow minimum of 3.58 cm^3 K mol^{-1} at *ca.* 80 K, and then gradually increased up to 230 K. An abrupt change in $\chi_M T$ was observed at this temperature, above which the plot traces the horizontal line before irradiation.

The temperature-independent $\chi_M T$ values before and after irradiation followed by annealing at >230 K clearly demonstrate that the sample under these conditions is characteristic of a magnetically dilute d^5 Mn^{II} ion; both the diazo ligand **8** and the chemically quenched carbene ligand are insulating magnetic couplers. The temperature dependence ($T < 230$ K) of the $\chi_M T$ values after photolysis of $[Mn(hfac)_2 \cdot \mathbf{8}]$ is best interpreted in terms of the formation of a ferrimagnetic 1D chain formed by alternating units of triplet di(4-pyridyl)carbenes and d^5 Mn^{II} ions (Fig. 13). As the temperature is lowered,

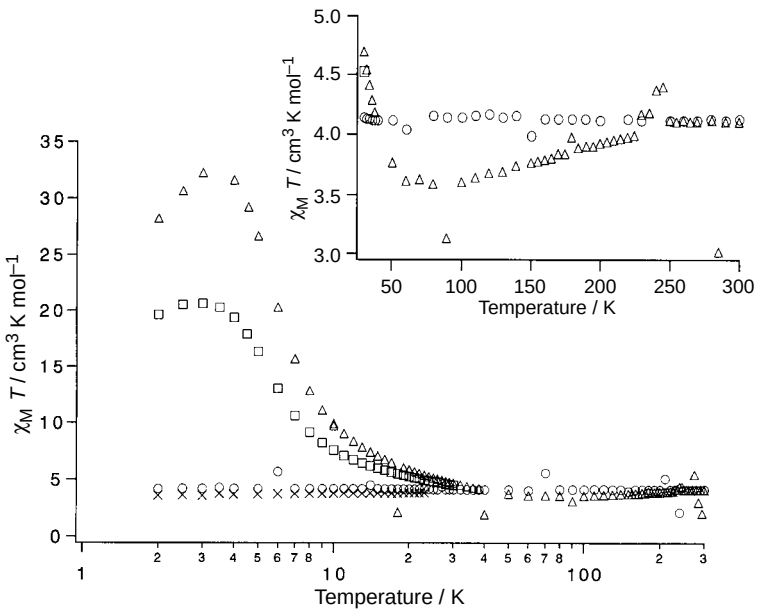

Fig. 12 Temperature dependencies of $\chi_M T$ for a crystalline sample of $[Mn(hfac)_2 \cdot \mathbf{8}]$: before (○) and after irradiation for 2 (□), 18 h (△), and then after being kept at 300 K for 1 h (×)

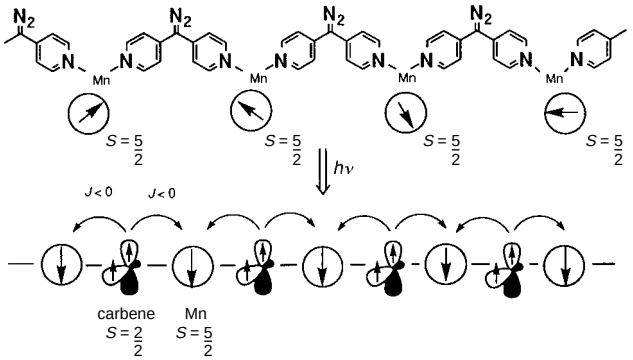

Fig. 13 Schematic representation of the formation of a 1D ferrimagnetic chain by photolysis of a dilute paramagnet [Mn(hfac)$_2$ · **8**]

the antiferromagnetic coupling of the unpaired electrons of the manganese ion ($S = \frac{5}{2}$) and the carbene center ($\frac{2}{2}$) becomes stronger than kT and produces a minimum in the $\chi_M T$ *vs.* T plot, as in a number of heterospin systems.[3] The correlation of increasing length along the ferrimagnetic chain leads to the increase in $\chi_M T$; the correlation length at 3 K is estimated to be the ordering over *ca.* 40 units. The decrease in $\chi_M T$ below 3 K is mostly due to antiferromagnetic interchain interaction and partly to the saturation of magnetization at the field of 500 Oe used for the measurement.

1D *Complex* [Cu(hfac)$_2$ · **8**] *before and after irradiation.* Before irradiation $\chi_M T$ values of a fine crystalline sample of [Cu(hfac)$_2$ · **8**] were nearly constant at 0.39 cm^3 K mol^{-1} in the range 2–300 K in good agreement with a theoretical spin-only value of 0.38 cm^3 K mol^{-1} for a dilute $S = \frac{1}{2}$ paramagnet. After photolysis, the $\chi_M T$ values increased steeply, reached a maximum at 3.0 K and then decreased monotonically as the temperature was increased. After an abrupt change at 230 K, the values traced exactly the temperature-independent data before irradiation, indicating that the triplet carbene units chemically transform back into diamagnetic products at temperatures above 230 K, clearly demonstrating that the di(4-pyridyl)carbene has a double role as a spin source and magnetic coupler.

Field dependency plots of magnetization of [Cu(hfac)$_2$ · **8**] before and after photolysis at 3.5 K were linear and convex curved, respectively. The latter was fitted to a Brillouin function in which $S = 26.4 \pm 0.2$. The ferromagnetic coupling between the Cu^{II} ion and the coordinated di(4-pyridyl)carbene is interpreted in terms of exchange coupling of the electrons in the mutually orthogonal $d_{x^2-y^2}$ atomic orbital of Cu and the π orbital on the pyridyl nitrogen which carries spin density due to the triplet carbene center at the *para* position.

Conclusions

Assemblage and alignment of electron spins of triplet bis(aminoxyl) and quartet tris(aminoxyl) radicals, *i.e.*, **1**–**7**, in macroscopic scale have been effectively achieved by using coordinatively doubly unsaturated paramagnetic 3d transition-metal ions as connectors. A divalent pyridine base **8** carrying a latent triplet center proved to be effectively assembled as well. The number and configuration of the coordination sites in the free radical ligands or precursor ligands control the dimensions of the magnetic structures of these metal–radical-ligand complexes. A clear-cut one-to-one correspondence has been found between tacticity of the extended molecular structures and dimension of the crystal structures; while the isotactic polymeric chains remain 1D and have difficulty in forming strong interchain interactions, as in [Mn(hfac)$_2$ · **1**], [Mn(hfac)$_2$ · **7** · n-C$_6$H$_{14}$] and [Mn(hfac)$_2$ · **8**], the syndiotactic chains have a tendency to grow into 2D ([{Mn(hfac)$_2$}$_3$ · **4**$_2$ · n-C$_7$H$_{16}$]) and/or 3D ([{Mn(hfac)$_2$}$_3$ · **7**$_2$]) networks by extending interchain connectivity.

The ligands we have employed so far are conformationally labile and chiral only in the crystal. The correct chirality of each ligand and the consequent tacticity have been selected during the self-assembling and crystallization processes. Furthermore, isotactic chains of opposite charality cancel each other out and there is no net chirality exhibited by the bulk crystals. Ongoing studies should employ ligands stable with respect to chirality to dictate the dimension of the resulting metal complexes. Once such crystals are obtained, they might have potential as chiral magnets that could show interesting photophysical behavior.

The paramagnetic complexes [Mn(hfac)$_2$ · **8**] and [Cu(hfac)$_2$ · **8**] afforded ferri- and ferro-magnetic 1D chains, respectively, when irradiated. It is worth noting that the carbene centers generated in these crystals survived temperatures as high as 200 K. Once a similar complex with a 3D structure is prepared and remnant magnetization is obtained at finite temperature, the system could serve as a photomagnetic recording device in which only the irradiated domain of the non- or weakly-magnetic materials becomes strongly magnetic, just as that of photoresists become functional for printing circuit elements.

The usefulness of the heterospin systems as versatile design agents for high T_C molecule-based magnetic materials would be increased by incorporation of the stereochemical aspect of chirality into the complex structures.[17]

Acknowledgements

This work was supported by a Grant-in-Aid for Scientific Research (No. 06453035) and a Grant-in-Aid for COE Research (#08CE2005) 'Design and Control of Advanced Molecular Assembly Systems' from the Ministry of Education, Science, Sports and Culture, Japan.

References

1 O. P. Anderson, *Inorg. Chem.*, 1980, **19**, 1417; J. R. Doedens, *Inorg. Chem.*, 1981, **20**, 2677.
2 M. Kitano, N. Koga and H. Iwamura, *J. Chem. Soc., Chem. Commun.*, 1994, 447; Y. Ishimaru, K. Inoue, N. Koga and H. Iwamura, *Chem. Lett.*, 1994, 1693; M. Kitano, Y. Ishimaru, K. Inoue, N. Koga and H. Iwamura, *Inorg. Chem.* , 1994, **33**, 6012.
3 G. R. Eaton and S. S. Eaton, *Acc. Chem. Res.*, 1988, **21**, 107; A. Caneschi, D. Gatteschi J. Laugier, P. Rey and R. Sessoli, *Inorg. Chem.*, 1988, **27**, 1553; A. Caneschi, D. Gatteschi, J. P. Renard, P. Rey and R. Sessoli, *Inorg. Chem.*, 1989, **28**, 1976; C. Benelli, A. Dei, D. Gatteschi, H. U. Gudel and L. Pardi, *Inorg. Chem.*, 1989, **28**, 3089; A. Caneschi, D. Gatteschi, R. Sessoli and P. Rey, *Acc. Chem. Res.*, 1989, **22**, 392; A. Caneschi, D. Gatteschi and P. Ray, *Prog. Inorg. Chem.*, 1991, **39**, 331; A. Caneschi, D. Gatteschi and R. Sessoli, in *Magnetic Molecular Materials*, eds. D. Gatteschi, O. Kahn, J. S. Miller and F. Palacio, NATO ARI Series E, Kluwer, Dordrecht, 1991, p. 215; A. B. Burdukov, V. I. Ovcharenko, V. N. Ikorski, N. V. Pervukhina, N. V. Podberezskaya, I. A. Grigor'ev, S. V. Larionov and L. B. Volodarsky, *Inorg. Chem.*, 1991, **30**, 972; A. Caneschi, A. Dei and D. Gatteschi, *J. Chem. Soc., Chem. Commun.*, 1992, 630; A. Caneschi, P. Chiesi, L. David, F. Ferraro, D. Gatteschi and R. Sessoli, *Inorg. Chem.*, 1993, **32**, 1445.
4 (*a*) K. Inoue and H. Iwamura, *J. Am. Chem. Soc.*, 1994, **116**, 3173; (*b*) K. Inoue and H. Iwamura, *J. Chem. Soc., Chem. Commun.*, 1994, 2273; (*c*) K. Inoue, T. Hayamizu and H. Iwamura, *Chem. Lett.*, 1995, 745; (*d*) T. Mitsumori, K. Inoue, N. Koga and H. Iwamura, *J. Am. Chem. Soc.*, 1995, **117**, 2467; (*e*) K. Inoue, T. Hayamizu, H. Iwamura, D. Hashizume and Y. Ohashi, *J. Am. Chem. Soc.*, 1996, **118**, 1803; (*f*) K. Inoue and H. Iwamura, *Adv. Mater.*, 1996, **8**, 73; (*g*) D. C. Oniciu, K. Matsuda and H. Iwamura, *J. Chem. Soc., Perkin 2*, 1996, 907; (*h*) K. Inoue and H. Iwamura,

Mat. Res. Soc. Symp. Proc., 1996, **413**, 313; (*i*) T. Hayamizu, K. Inoue and H. Iwamura, unpublished work.
5 G. Brand, M. W. Hosseini, O. Felix, P. Schaffer and R. Ruppert, in *Magnetism: A Supramolecular Function*, ed. O. Kahn, NATO ASI Series C, Kluwer, Dordrecht, 1996, p 129.
6 The original formulation of this strategy appeared in: K. Inoue, T. Hayamizu and H. Iwamura, *Mol. Cryst. Liq. Cryst.*, 1995, **273**, 67; H. Iwamura, K. Inoue and T. Hayamizu, *Pure Appl. Chem.*, 1996, **68**, 243; H. Iwamura, K. Inoue, N. Koga and T. Hayamizu, in *Magnetism: A Supramolecular Function*, ed. O. Kahn, NATO ASI Series C, Kluwer, Dordrecht, 1996, p 157.
7 (*a*) A. Calder, A. R. Forrester, P. G. James and G. R. Luckhurst, *J. Am. Chem. Soc.*, 1969, **91**, 3724; (*b*) K. Mukai, H. Nagai and K. Ishizu, *Bull. Chem. Soc. Jpn.*, 1975, **48**, 2381; (*c*) F. Kanno, K. Inoue, N. Koga and H. Iwamura, *J. Phys. Chem.*, 1993, **97**, 13267.
8 T. Ishida and H. Iwamura, *J. Am. Chem. Soc.*, 1991, **113**, 4238.
9 (*a*) C. Murray and C. Wentrup, *J. Am. Chem. Soc.*, 1975, **97**, 7467; (*b*) M. Ono, M.Sc. Thesis, The University of Tokyo, 1991.
10 N. Koga, Y. Ishimaru and H. Iwamura, *Angew. Chem., Int. Ed. Engl.*, 1996, **35**, 755.
11 (*a*) H. M. McConnell, *J. Chem. Phys.*, 1963, **39**, 1910; (*b*) A. Izuoka, S. Murata, T. Sugawara and T. Iwamura, *J. Am. Chem. Soc.*, 1987, **109**, 2631; (*c*) K. Yamaguchi, Y. Toyoda and T. Fueno, *Chem. Phys. Lett.*, 1989, **159**, 459.
12 C. Zheng and R. Hoffmann, *Inorg. Chem.*, 1989, **28**, 1074.
13 B. Bleaney and K. D. Bowers, *Proc. Royal Soc. London*, 1952, **A214**, 451.
14 J. Fujita, M. Tanaka, H. Suemune, N. Koga, K. Matsuda and H. Iwamura, *J. Am. Chem. Soc.*, 1996, **118**, 9347.
15 W. E. Hatfield and K. L. Trojan, in *Research Frontiers in Magnetochemistry*, ed. C. J. O'Connor, World Scientific, Singapore, 1993, pp. 1–26; E. Coronado, M. Drillon and R. Georges, *ibid.*, pp. 27–66; D. Gatteschi and L. Pardi, *ibid.*, pp. 67–86.
16 M. Hitzfeld, P. Ziemann, W. Buckel and H. Claus, *Phys. Rev. B*, 1984, **29**, 5023; *Phys. Rev. B*, 1984, **29**, 5023; O. Kahn., in *Organic and Inorganic Low-Dimensional Crystalline Materials*, Delhaes P., Drillon M., eds., NATO ASI Series 168, Plenum, New York, 1987, p. 93.
17 S. Decurtins, R. Pellaux, A. Hauser and M. E. von Arx, in *Magnetism: A Supramolecular Function*, ed. O. Kahn, NATO ASI Series C, Kluwer, Dordrecht, 1996, p 487.

Received 27*th January* 1997; *Paper* 7/07641J